Macroscopic Na$^+$ Currents in the "Nonconducting" *Shaker* Potassium Channel Mutant W434F

JOHN G. STARKUS,*‡ LIOBA KUSCHEL,* MARTIN D. RAYNER,§ and STEFAN H. HEINEMANN*

From the *Max-Planck Society, Research Unit Molecular and Cellular Biophysics, D-07747 Jena, Germany; ‡Békésy Laboratory of Neurobiology, Pacific Biomedical Research Center, and §Department of Genetics and Molecular Biology, School of Medicine, University of Hawaii, Honolulu, Hawaii 96822-2359

ABSTRACT C-type inactivation in *Shaker* potassium channels inhibits K$^+$ permeation. The associated structural changes appear to involve the outer region of the pore. Recently, we have shown that C-type inactivation involves a change in the selectivity of the *Shaker* channel, such that C-type inactivated channels show maintained voltage-sensitive activation and deactivation of Na$^+$ and Li$^+$ currents in K$^+$-free solutions, although they show no measurable ionic currents in physiological solutions. In addition, it appears that the effective block of ion conduction produced by the mutation W434F in the pore region may be associated with permanent C-type inactivation of W434F channels. These conclusions predict that permanently C-type inactivated W434F channels would also show Na$^+$ and Li$^+$ currents (in K$^+$-free solutions) with kinetics similar to those seen in C-type-inactivated *Shaker* channels. This paper confirms that prediction and demonstrates that activation and deactivation parameters for this mutant can be obtained from macroscopic ionic current measurements. We also show that the prolonged Na$^+$ tail currents typical of C-type inactivated channels involve an equivalent prolongation of the return of gating charge, thus demonstrating that the kinetics of gating charge return in W434F channels can be markedly altered by changes in ionic conditions.

KEY WORDS: potassium channels • channel inactivation • ion selectivity • patch clamp • channel gating

INTRODUCTION

Shaker potassium channels (K$^+$ channels) respond to membrane depolarizations by conformational changes that open a permeation pathway that is highly selective for K$^+$ over Na$^+$. However, K$^+$ channels are capable of conducting substantial Na$^+$ currents when K$^+$ ions are removed from the bathing media (Korn and Ikeda, 1995). In addition, a point mutation in the putative pore region of the channel protein (W434F) results in channels that do not conduct ions to any appreciable extent under physiological situations, but leave the gating currents, resulting from voltage-sensor movements, largely intact (Perozo et al., 1993). This mutation has gained considerable recognition since it has proved useful for studying gating currents in the absence of signal-contaminating ionic currents.

Recently, Yang et al. (1997) shed further light on the nature of W434F-mutated *Shaker* channels by showing that these channels appear C-type inactivated at depolarized voltages. Tandem tetrameric constructs were formed using "wild-type" *Shaker* monomers linked to either one or two *Shaker* monomers containing the W434F mutation. Both monomer types had NH$_2$-terminal deletions to remove fast inactivation. Injection of these tetrameric construct RNAs in *Xenopus* oocytes yielded channels that can be predicted to contain either one or two W434F monomers. Yang et al. (1997) noted that the rate of C-type inactivation increased in proportion to the number of W434F monomers per channel and concluded that the homomultimeric W434F channel should be effectively C-type inactivated at depolarized membrane potentials.

The kinetics of C-type inactivation in wild-type *Shaker* channels are strongly influenced by the extracellular concentrations of K$^+$ and other permeant ions (Lòpez-Barneo et al., 1993). Furthermore, entry into the C-type inactivated state appears to involve protein conformational rearrangements at the extracellular entry of the channel pore (Liu et al., 1996; Schlief et al., 1996). In a previous report (Starkus et al., 1997), we showed that C-type inactivated *Shaker* channels appear impermeable to K$^+$ ions, although they continue to conduct Na$^+$ (and Li$^+$) ions in K$^+$-free internal solutions. In these solutions, Na$^+$ tail currents are initially fast but become markedly slowed as C-type inactivation develops over time. The fast tail peak disappears while the slow component increases in direct proportion to the fraction of channels entering into C-type inactivation. Meanwhile,

the selectivity filter appears to change its properties, sharply reducing K$^+$ permeation but allowing continued Na$^+$ permeation as channels enter C-type inactivated states. This conclusion, that the primary mechanism of C-type inactivation involves structural changes that alter the properties of the selectivity filter, contrasts markedly with conventional expectations that all forms of "inactivation" should reflect blockade, or collapse, of the ion permeation pathway.

Since the results of Yang et al. (1997) had indicated that W434F mutant channels are C-type inactivated at depolarized potentials, we explore here the prediction that W434F mutant channels, in the absence of K$^+$, should show Na$^+$ permeation with slow activation and deactivation kinetics similar to those found under equivalent ionic conditions in C-type inactivated wild-type *Shaker* channels (see Starkus et al., 1997). The results presented here are in accord with that prediction, and thus appear to support the conclusion that the W434F mutant may be inherently or permanently C-type inactivated. However, a more direct and equally significant conclusion from our data is that W434F channels can conduct significant macroscopic currents in appropriate solutions. Thus, the activation and deactivation kinetics of W434F channels can be directly assayed for comparison with gating charge movements.

MATERIALS AND METHODS

Channel Expression

Control data for this study were obtained using the *Shaker* 29-4 construct (Iverson and Rudy, 1990) in which fast (N-type) inactivation was removed by deletion of the residues 2–29 (McCormack et al., 1994); this construct will be referred to as *Sh*Δ. We also used a W434F mutation created in this same *Sh*Δ background. Oocytes of *Xenopus laevis* were surgically obtained under tricaine/ice water anesthesia. Follicular layers were removed according to standard methods. mRNA was synthesized in vitro and injected into *Xenopus* oocytes at a concentration ranging between 0.005 and 0.1 μg/μl per oocyte (50 nl). Oocytes were incubated at 18°C for 1–7 d before electrophysiological recordings.

Electrophysiology

All data were obtained in inside-out macro-patch recordings (Hamill et al., 1981) using either an EPC-7 or EPC-9 patch-clamp amplifier (HEKA Elektronik, Lambrecht, Germany). Patch pipettes were fabricated from aluminum silicate or borosilicate glass, yielding resistances in standard solutions between 0.5 and 2 MΩ. Data acquisition was controlled with the Pulse+PulseFit software package (HEKA Elektronik). Experiments were carried out at room temperature ranging between 20 and 22°C. Data analysis was performed with PulseFit, PulseTools (HEKA Elektronik), and IgorPro (Wave Metrics, Lake Oswego, OR) software. Leak and capacitive transients were compensated using a variable P/n correction (Heinemann et al., 1992) with a typical leak holding potential of −120 mV. In several cases, leak and capacitive transients were eliminated by off-line leak correction methods. Unless stated otherwise, data values are specified as mean ± SD (n = number of independent experiments).

Where appropriate, estimates of the effective voltage sensitivity of transitions in the activation or deactivation pathways were obtained by fitting the time constant according to

$$\tau(V) = \tau(0) \exp(\pm Vq/kT), \tag{1}$$

where $\tau(V)$ is the observed time constant at the applied transmembrane voltage, V, k is Boltzmann's constant, T is the absolute temperature, and q is the apparent charge moved between the appropriate thermodynamic energy well and the energy barrier for the transition in question.

Double-exponential fits were applied to ionic current data by fitting the time course of the ionic tail currents, $I(t)$, to the following equation:

$$I(t) = a_0 + a_f \exp(-t/\tau_f) + a_s \exp(-t/\tau_s), \tag{2}$$

where a_0 is the predicted steady state current, a_f and a_s are the zero time intercepts of the first and second exponential components, and τ_f and τ_s are the corresponding time constants for these components.

Solutions

As all patch-clamp experiments were done in the inside-out configuration, only the intracellular bath solution could be changed for individual patches. Solution changes were carried out by exposing the patch pipette tips to a constant stream of bath solution applied over a quartz capillary manifold operated by magnetic valves. Great care had to be taken in carrying out solution exchanges to ensure effective removal of residual K$^+$ from earlier bath solutions, from close proximity of the patch to the oocyte surface, or from cytoplasm adhering to a freshly excised inside-out patch. For rapid solution changes (see Fig. 2), a piezo-driven double-barrel pipette (Θ-glass) was used. The patch pipette was positioned such that its tip was exposed to the solution stream from the left or right barrel of this application pipette.

In addition to monovalent chloride salt, external solutions always contained 1.8 mM CaCl$_2$ and 10 mM HEPES (pH 7.2). Internal solutions contained 1.8 mM EGTA and 10 mM HEPES (pH 7.2). The solutions were named according to the content of monovalent cations containing (mM): Normal Frog Ringer, 115 NaCl, 2.5 KCl; K-Ringer, 115 KCl; Na-Ringer, 115 NaCl; Li-Ringer, 115 LiCl; Tris-Ringer, 115 TrisCl; K-EGTA, 115 KCl; Na-EGTA, 115 NaCl; Tris-EGTA, 115 TrisCl.

Combinations of these monovalent cations were obtained by appropriate mixing of the solutions. In the text and figures, the solutions are only specified by the concentrations of the monovalent cations: external//internal solution.

RESULTS

Na$^+$ Ions Permeate through W434F Channels

In Fig. 1, data traces are shown from both *Sh*Δ and W434F channels in the presence (*left*) and absence (*right*) of K$^+$ ions where Na$^+$ is the only permeant ion. Fig. 1 *B* clearly indicates the well-known property of the W434F mutation, namely that it completely suppresses ionic conduction, clearly exposing ON and OFF gating currents. In the right panels, where the calculated Na$^+$ reversal potential is +28 mV, a step to +20 mV generates clearly visible ON gating currents, IgON, followed by only very small inward Na$^+$ currents. However, large OFF currents are visible in both *Sh*Δ (Fig. 1 *C*) and
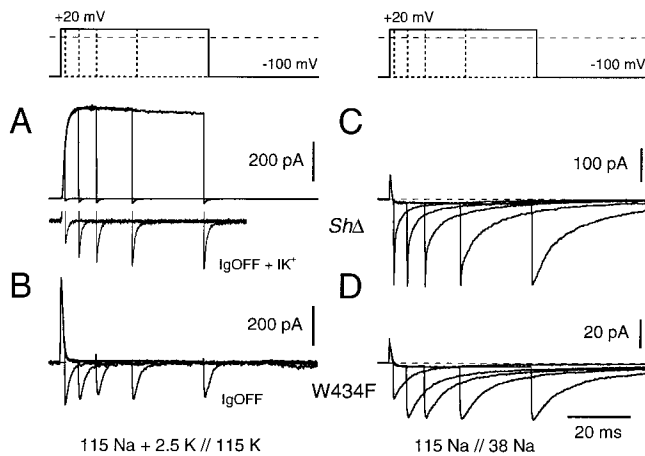
FIGURE 1. W434F channels conduct Na$^+$ ions in the absence of internal K$^+$. (*A–D*) Inside-out macropatch currents from oocytes expressing inactivation-removed *Sh*Δ and W434F channels were evaluated in K$^+$-containing (*left*) and K$^+$-free Na$^+$ (*right*) solutions. (*A*) In physiological solutions, *Sh*Δ channels conduct K$^+$ currents. To permit kinetic comparisons with records in different ionic conditions, the tail current sections of these traces have been magnified 10-fold (*inset*). (*B*) The W434F mutant in the presence of K$^+$ ions does not permit ionic current, thus exposing only the ON and OFF gating charge movements. (*C*) Kinetics of the Na$^+$ tail currents from *Sh*Δ channels in K$^+$-free solutions show a strong dependence on test pulse duration (Starkus et al., 1997). The fast tail currents seen at the shortest test pulse durations convert to slow tail currents as test pulse duration is increased. (*D*) W434F channels do not undergo marked alterations in kinetics as test pulse duration is increased, as would be expected if these channels are permanently C-type inactivated. The W434F Na$^+$ tail currents are strikingly similar in their kinetics to the *Sh*Δ tail currents after the longest test pulse duration shown here (64 ms). All traces were digitally low-pass filtered at 1 kHz.

W434F (Fig. 1 *D*) channels. Integration of these OFF currents indicates that they are many-fold larger than the IgON integrals, confirming the presence of substantial ionic currents that can only be carried by Na$^+$ in these K$^+$-free solutions. Thus, it is evident that Na$^+$ conduction occurs through both *Sh*Δ channels and nonconducting W434F channels in K$^+$-free solutions. Additionally, after the longest test pulses used here (64 ms, Fig. 1, *C* and *D*), both *Sh*Δ and W434F channels show rather similar slow tail current kinetics. Although this initial view confirms the key predictions of our study, there is much additional information in this figure that is addressed below.

First, we consider the records from *Sh*Δ channels in both physiological (Fig. 1 *A*) and Na$^+$ (Fig. 1 *C*) solutions. Where K$^+$ ions are present (Fig. 1 *A*), large outward K$^+$ currents are followed by small deactivating inward currents. These inward K$^+$ currents were generated by returning to −100 mV after various durations at a test potential of +20 mV. Since the calculated K$^+$ reversal potential is −96 mV, the deactivating K$^+$ currents

are very small at this return potential and may be substantially contaminated with unsubtracted IgOFF. To permit visual comparison of these small currents with the equivalent Na$^+$ current records shown in Fig. 1 *C*, a magnified version of the inward current section of these traces is also shown (Fig. 1 *A, inset*). This comparison indicates a marked difference between the simple, apparently mono-exponential, deactivating currents of Fig. 1 *A* from noninactivated channels and the more complex deactivating currents of Fig. 1 *C*. In a previous paper (Starkus et al., 1997), we have shown that this complexity arises from the development of C-type inactivation, which is very fast in K$^+$-free solutions, equilibrating in 50–100 ms (see also Kiss and Korn, 1998), as compared with a time course of several seconds in physiological solutions.

Integration of IgON yields an ON gating charge of ∼65 fC in all traces of Fig. 1 *C*, and the first trace after a 2-ms test pulse shows a dominant time constant of 3.8 ms and yields a total charge movement of ∼1.0 pC. Hence, IgOFF is only ∼6% of the charge moved in this trace, and 94% results from Na$^+$ current. By contrast, after a 64-ms test pulse, the initial fast component is lost and the dominant deactivation time constant is now 33 ms. Since total charge moved is here 5.8 pC, ∼99% of the total OFF signal must derive from ionic current. From here on, we shall refer to these deactivating currents as fast and slow Na$^+$ tail currents, respectively, since they result, primarily, from ionic currents. In K$^+$-free solutions, the development of C-type inactivation is linearly related to the loss of the fast Na$^+$ tail current component and to the increase in the amplitude of the slow deactivating component. We concluded that the fast tail current component is carried through noninactivated channels and that the slow Na$^+$ tail current arises from C-type inactivated channels. Therefore, as shown in Fig. 1 *C*, C-type inactivation is essentially complete following a 64-ms test pulse (*last trace*) in K$^+$-free Na$^+$ solutions, as is indicated by the disappearance of the fast tail current component in this record.

The equivalent pulse protocols and ionic conditions were repeated for mutant W434F. In physiological solutions (Fig. 1 *B*), no outward K$^+$ current is detectable at test potential, and only the ON gating current at +20 mV and the OFF gating currents at −100 mV are apparent. Integrations of these IgON and IgOFF signals yielded identical charge measurements, thus confirming the absence of ionic conduction in K$^+$-containing solutions, as previously reported by Perozo et al. (1993). By contrast, in K$^+$-free solutions where Na$^+$ is the only permeant ion (see Fig. 1 *D*), slow Na$^+$ tail currents are visible. These Na$^+$ tail currents show no initial fast component and are kinetically similar at all test pulse durations, as would be expected if W434F channels are per-

manently C-type inactivated. (However, the tail current at the shortest pulse duration shows a faster deactivation rate, indicating some time dependence of the deactivation kinetics, even in W434F channels.) In addition, these tail currents are kinetically similar to $Sh\Delta$ tail currents (see Fig. 1 C), once the $Sh\Delta$ channels have reached a steady state level of C-type inactivation (after ~60 ms).

In the absence of NH_2-terminal inactivation, C-type inactivation is readily characterized in $Sh\Delta$ channels from the inactivation of K^+ currents. However, see Fig. 1 B (and also Perozo et al., 1993); in the nonconducting W434F mutant no macroscopic K^+ currents are detectable. Some alternative measure must, therefore, be used when assessing C-type inactivation in the W434F mutant. Since development of C-type inactivation could, potentially, be either very fast or extremely slow in W434F channels, it seems particularly important to select an indirect indicator that has been shown to track the C-type inactivation of macroscopic currents across a wide range of onset rates. The primary indicator used here, the presence of slow Na^+ tail currents, meets this criterion. As noted by Starkus et al. (1997), the slow tails develop within ~60 ms in K^+-free solutions where C-type inactivation is also complete by this time (see their Fig. 2); furthermore, in 2.5 mM external K^+ solution where C-type inactivation requires several seconds to become fully equilibrated, the onset of C-type inactivation is still linearly related to the rate of development of the slow tail current component (see their Fig. 3, C–E).

K^+ Ions Block Na^+ Permeation and Affect Estimates of Relative Permeabilities

We previously demonstrated (Starkus et al., 1997) that K^+ ions can block Na^+ permeation through C-type inactivated channels in $Sh\Delta$. We therefore tested whether a similar blocking effect by internal K^+ would also occur in the permanently C-type inactivated mutant, W434F. A fast perfusion system was positioned in front of an excised inside-out patch so that internal K^+ could be added or subtracted during a maintained pulse to +50 mV within a few milliseconds (Fig. 2). With 5 mM K^+ plus 110 Na on the inside, it is clear that no outward Na^+ conduction occurs through the W434F channel. After removing internal K^+ ions, the outward Na^+ current appears and then disappears when 5 mM K^+ is added back to the internal solution (Fig. 2 A). In Fig. 2 B, the sequence of ionic changes was reversed. The same patch was first exposed to K^+-free solution in which an outward Na^+ current appears. This current was then blocked by adding internal K^+ ions and the Na^+ current reappeared when K^+ ions were removed. Since Na^+ Ringer was used on the external side of the membrane, a substantial Na^+ tail current was generated at the end of this pulse. However, this Na^+ tail cur-
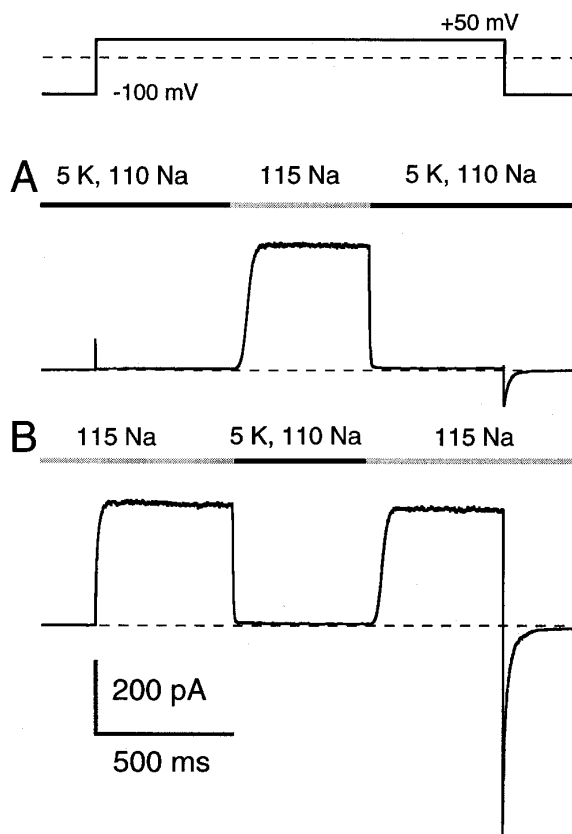

FIGURE 2. Internal K^+ ions block Na^+ conduction through W434F channels. A fast perfusion system allowed rapid changes of internal solutions during a maintained depolarizing pulse to +50 mV. Changes in the ionic conditions are displayed above the current traces. (A) Na^+ current is blocked when the internal surface of the patch is exposed to 5 mM K^+. When internal K^+ is replaced with Na^+ ions, the patch conducts outward Na^+ current. This current is then blocked by return of internal K^+ ions. (B) Channels are first exposed only to internal Na^+ ions yielding outward Na^+ currents. When K^+ ions are added, Na^+ conduction is blocked. This block is relieved when K^+ ions are again removed. Since 115 mM Na^+ Ringer was used as the external solution, a large Na^+ tail current is observed when the patch was repolarized to −100 mV. The difference in kinetics of the current response to washin and washout of internal K^+ indicates that much smaller K^+ concentrations than 5 mM are sufficient to block Na^+ currents through W434F channels.

rent can be blocked by 5 mM K^+, as shown by the small OFF current in Fig. 2 A.

Since K^+ ions block Na^+ conduction through both noninactivated channels (Korn and Ikeda, 1995) and C-type inactivated channels (Starkus et al., 1997), the relative permeabilities measured in standard bi-ionic conditions where K^+ is the internal reference ion must reflect this K^+ block. This problem becomes acute in C-type inactivated channels where K^+ ions are essentially impermeant. Fortunately, using a pulse protocol and ionic solutions equivalent to those of Fig. 1, it is simple to demonstrate even low levels of ion permeation in

tail currents by comparison of ON and OFF integrals. We have found significant permeation for Na^+ ions (see Fig. 1) as well as for Li^+ and NH_4^+ (data not shown), but no significant permeation was detectable for K^+, Cs^+, or Rb^+ ions. This pattern is similar to that reported by Starkus et al. (1997), who showed permeation by Na^+ and Li^+ ions in C-type inactivated $Sh\Delta$ channels but no detectable permeation by K^+ ions.

Activation and Deactivation Parameters of Na^+ Currents in W434F

Families of Na^+ currents through W434F channels were obtained across a wide range of voltages, as shown in Fig. 3, *A* and *B*. Although the relative permeability for Na^+ ions is high, the absolute permeability for Na^+ is low in these channels and may be slightly less than the Na^+ permeability of C-type inactivated $Sh\Delta$ channels (see Fig. 1, *C* and *D*). Therefore, for these experiments, the ionic conditions were adjusted to maintain a substantial driving force for Na^+ ions through the W434F channels. For negative test potentials, inward currents (Fig. 3 *A*) were obtained using external Na-Ringer and internal Tris-EGTA. For positive test potentials, outward current records (Fig. 3 *B*) were obtained using Tris-Ringer externally and internal Na-EGTA. In both panels, Na^+ was the only permeant cation, and current direction is determined by the direction of the Na^+ gra-

dient, again confirming that these currents are carried by Na^+ ions.

The voltage sensitivity of the fast and slow activation time constants for Na^+ currents through W434F channels is illustrated in Fig. 3 *C*. As shown in the data traces, both the small ($\bullet$) and large ($\circ$) activation time constants are quite steeply voltage sensitive for the inward currents at negative test potentials; however, these time constants become relatively voltage insensitive for the outward currents at positive voltages. When P_{open} is plotted as a function of voltage (see Fig. 3 *D*), it is apparent that the region in which activation rates change with potential coincides with the potential range over which P_{open} is changing in response to test potential. Similarly, at positive test potentials where activation time constants seem relatively insensitive to changes in test potential, we note that P_{open} is already saturated.

As noted above, Fig. 3 *D* shows the steady state activation curve for W434F channels ($\circ$) obtained by plotting normalized peak tail currents (at -100 mV) against test potential, following 500-ms pulses to test potential. The midpoint of steady state activation (50% activation) in C-type inactivated W434F channels is $\sim$10 mV left-shifted by comparison with steady state activation curves from noninactivated $Sh\Delta$ channels ($\blacksquare$) in symmetric K^+ solutions.

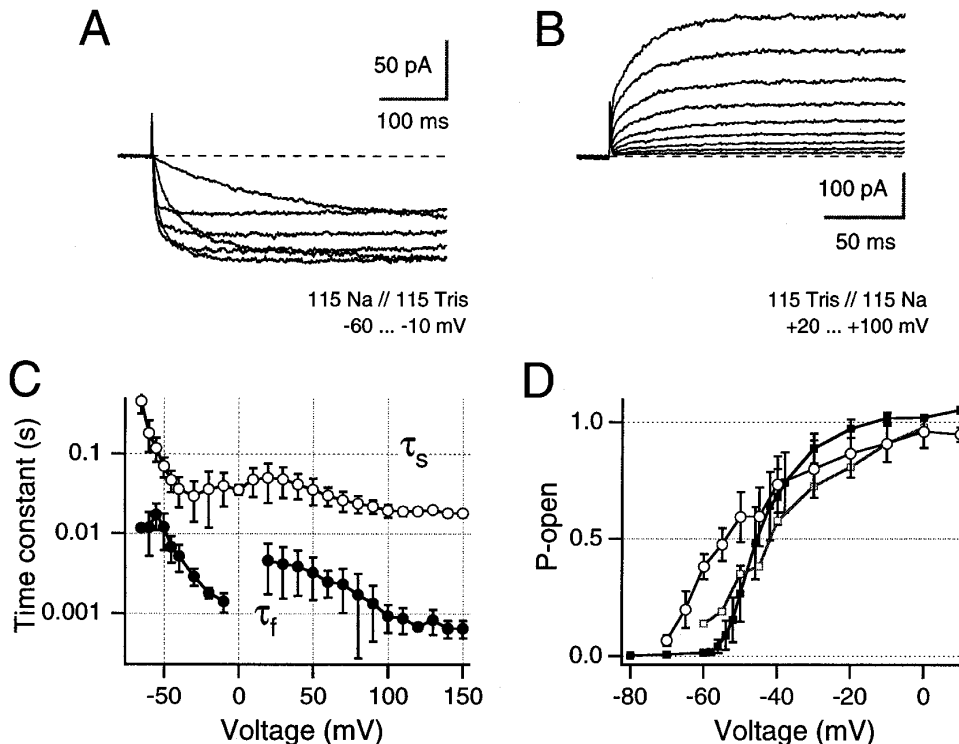Finally, as shown in Fig. 4, kinetic analysis confirms

FIGURE 3. Activation kinetics of Na^+ currents through W434F channels. (*A*) Inside-out current recordings with asymmetrical 115 Na//115 Tris solutions in response to depolarizations ranging from -60 to -10 mV. (*B*) Current traces elicited by voltage steps ranging from $+20$ to $+100$ mV using an inverted Na^+ gradient: 115 Tris//115 Na. Holding potential in *A* and *B* was -100 mV. (*C*) The time course of activation was described by double-exponential data fits (Eq. 2). The resulting time constants of the fast (τ_f, $\bullet$) and slow (τ_s, $\circ$) components are plotted as a function of the test potential. The data points were connected with straight lines. (*D*) The normalized open-probability after depolarizations for 500 ms was plotted as a function of the test potential. ($\circ$) W434F in Na//Na solutions, ($\square$) C-type inactivated $Sh\Delta$ in symmetrical Na//Na solutions, ($\blacksquare$) noninactivated $Sh\Delta$ in K//K solutions. All data points are mean $\pm$ SD, $n = 9$–14.
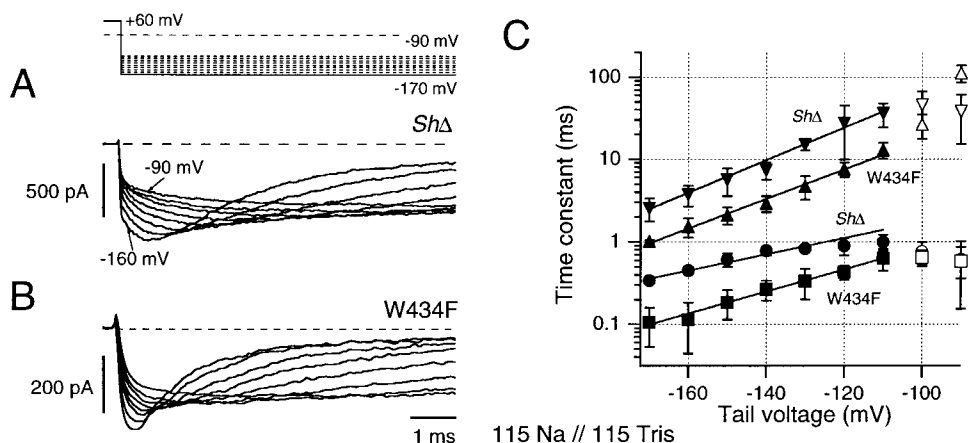
FIGURE 4. Kinetics of tail current deactivation in W434F channels. Na$^+$ tail currents from C-type inactivated $Sh\Delta$ (*A*) and W434F (*B*) channels are compared. All data traces are from inside-out patches in asymmetrical 115 Na//115 Tris solutions. Patches were depolarized for 100 ms at +60 mV; the subsequent tail voltages ranged from −90 to −170 mV. (*C*) Deactivation time course was described by the sum of two exponential functions. Fits were started 200 μs after the start of the hyperpolarization step to avoid the open-channel currents associated with the rising phase of the voltage clamp. The resulting mean time constants are plotted as a function of the tail voltage. The symbols for the rising phase are (*circles*) $Sh\Delta$ and (*squares*) W434F. The symbols for the falling phase are (*downward triangles*) $Sh\Delta$ and (*upward triangles*) W434F. The data points indicated by filled symbols were used for the estimation of the voltage dependencies according to Eq. 1. The resulting apparent gating charges are for $Sh\Delta$: q(rise) = 0.57 e$_0$, q(fall) = 1.15 e$_0$; for W434F: q(rise) = 0.78 e$_0$, q(fall) = 1.04 e$_0$. All data points are mean ± SD, n = 5 patches.

the apparent similarity noted above in the Na$^+$ tail current kinetics for W434F channels and C-type inactivated $Sh\Delta$ channels. Representative tail currents from $Sh\Delta$ (Fig. 4 *A*) and W434F (Fig. 4 *B*) are shown here for comparison of kinetics. Data traces from five patches were analyzed by double-exponential fitting to the rising and falling phase of the tail currents. Although the falling phase is clearly double exponential in both channels, we here present data only for the two faster components, a rising phase and the fast falling phase. Fig. 4 *C* shows mean time constants obtained for both the "hooked" rising phase (*circles, $Sh\Delta$; squares*, W434F) and the fast falling phase (*inverted triangles, $Sh\Delta$; upright triangles*, W434F), plotted as a function of the return potential. Although the deactivation kinetics for W434F channels appear to be consistently approximately two-fold faster than for $Sh\Delta$, the similarities in both voltage sensitivity and rate again indicate that both channel types are C-type inactivated under the conditions of these experiments.

In conclusion, despite small quantitative differences between W434F and C-type inactivated $Sh\Delta$ channels, there are broad similarities between the characteristics of Na$^+$ current activation and deactivation in these two channel types. Thus, the slow kinetics of Na$^+$ current activation in W434F channels seem consistent with previous conclusions that W434F channels are C-type inactivated under these conditions.

Return of Gating Charge Is Affected by Ionic Conditions in W434F Channels

In *Shaker* channels, tail current time constants have been shown to be affected by the nature of the permeant ion (Zagotta et al., 1994), with change from K$^+$

permeation to Rb$^+$ permeation leading to an approximately fivefold slowing of the deactivation rate. Similarly, Starkus et al. (1997) have shown that tail current deactivation rate is also affected by the channel state; specifically, entry into C-type inactivated states slows deactivation (see also Fig. 1 *C*). However, it has been considerably more difficult to show whether either ionic conditions or channel state can affect the kinetics of Ig-OFF. If W434F channels are permanently C-type inactivated under normal experimental conditions, then it should be possible to obtain direct comparisons between IgOFF rates under different ionic conditions without the confounding variable of change in channel state.

In W434F channels, preliminary comparisons between the rate of charge return, IgOFF, in K$^+$-containing solutions (Fig. 1 *B*) and the ionic current deactivation rate in K$^+$-free Na$^+$ solutions (Fig. 1 *D*) shows that these rates are very different. This finding seems consistent with the dissociation between OFF gating current and tail current kinetics, noted by Bezanilla and Stefani (1994). Alternatively, in our data, the difference in rates might be partially or fully explained by the difference in ionic conditions (see also Chen et al., 1997). This question is directly addressed in Fig. 5.

Fig. 5 demonstrates the results of an experiment in which OFF charge return is evaluated from the recovery of IgON in a double-pulse protocol with varying interpulse intervals, while tail current kinetics are evaluated directly from the deactivation of ionic current. The holding and return potentials were at −100 mV and test pulses were to +20 mV. In Fig. 5 *A*, only the ON and OFF gating currents occur since the inward Na$^+$ current is blocked here by high concentrations of internal K$^+$ ions. In the presence of K$^+$ ions and the ab-

+20 mV

-100 mV

A

20 pA

115 Na + 2.5 K // 115 K

B

10 pA
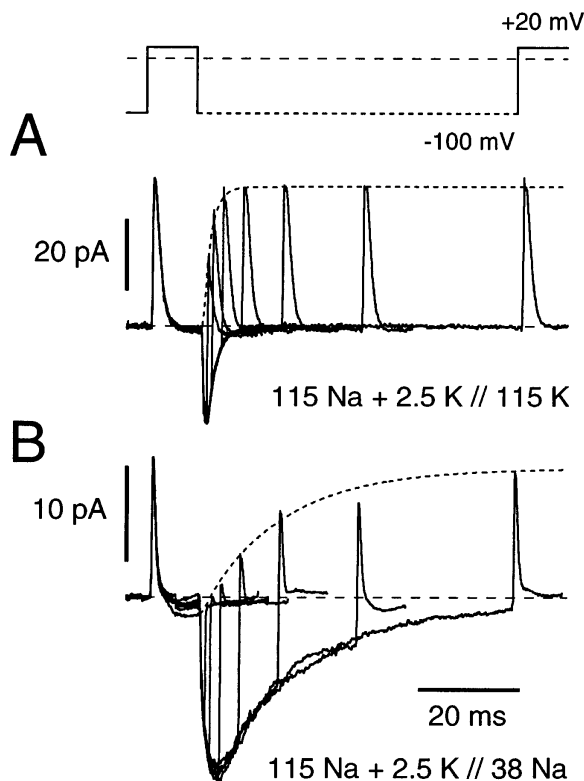
20 ms

115 Na + 2.5 K // 38 Na

FIGURE 5. The rate of gating charge return in W434F channels is affected by ionic conditions. Double-pulse protocols with variable interpulse intervals were used to assess the kinetics of gating charge return by observing the recovery of IgON in the second pulse. (A) In the presence of internal K⁺, only gating currents are observed and recovery of peak IgON in the second pulse follows the falling phase kinetics of IgOFF. (B) In a K⁺-free internal Na⁺ solution, IgON shows an initial delay in recovery that coincides with the rising phase of the ionic tail current. This is followed by a recovery phase in which IgON peaks increase with a time course that parallels the deactivation phase of the ionic tail current. For dashed curves see text.

sence of Na^+ permeation, the return of OFF charge exactly parallels the rate of recovery of IgON. However, the rate of charge return in Fig. 5 B is much slower when internal K^+ ions are absent and Na^+ ions are permeating through the pore. In Fig. 5 B, the inward Na^+ tail currents are supported by a high driving force, although the ionic current during the test pulse is very small since the test potential (+20 mV) is very close to the theoretical reversal potential of +28 mV in these solutions. Thus, IgON is clearly visible during the first and second test pulses. When the inward tail current is compared with the recovery of IgON, it is apparent (a) that there is an initial delay in charge return corresponding to the slowed rising phase of the "hooked" tail current, (b) that the deactivation rate of the ionic current closely parallels the rate of recovery of peak IgON, and (c) that the rate of charge return is slower under ionic conditions that support Na^+ permeation.

These conclusions are supported by kinetic measurements. The dashed curves fitted to the peaks of IgON were obtained from double-exponential fits to the IgOFF (Fig. 5 A) or the tail current (Fig. 5 B). These fits gave rising phase time constants of 0.5 (Fig. 5 A) and 1.0 (Fig. 5 B) ms, and falling phase time constants of 1.6 (Fig. 5 A) and 16 (Fig. 5 B) ms. These values were then used to simulate the initial delay and recovery of IgON, as shown in the dashed curves, which were then scaled to the final values of IgON.

While these findings clearly demonstrate that OFF charge movements are affected by ionic conditions, the exact cause of this change in IgOFF rates is not yet clear. One possibility would be that permeating Na^+ ions interact with C-type inactivated channels in such a way as to delay charge return. An alternative possibility would be that internal K^+ ions bind to a highly K^+-selective regulatory site and that the absence of K^+ ions at this site slows the rate of both charge return and channel deactivation. In either case, however, our findings suggest a tight coupling between the rates of OFF charge return and ionic current deactivation in W434F channels.

DISCUSSION

Principal Findings

(a) Ionic currents can be readily demonstrated through excised patches expressing W434F channels, provided that K^+ ions are first removed from the internal side of the membrane (see Fig. 1 D). As shown in Fig. 3, A and B, where the only potentially permeant cations are Na^+ (115 mM, internal or external) and Ca^{2+} (1.8 mM, external only), the direction of the observed currents is fully determined by the direction of the Na^+ gradient. Thus, it is clear that the currents seen here must be carried by Na^+ ions.

(b) By contrast, no detectable ionic current occurs through W434F channels when these channels are examined in physiological media containing internal K^+ ions (Fig. 1 B). The Q_{OFF}/Q_{ON} ratio is essentially unity in K^+-containing solutions, and it is clear that neither Na^+ ions (115 mM externally) nor K^+ ions are significantly permeant in the presence of physiological K^+ concentrations. The effectiveness of K^+ block by as little as 5 mM internal K^+ is demonstrated in Fig. 2. These results are consistent with previous studies on W434F channels (Perozo et al., 1993; Bezanilla and Stefani, 1994). However, when ion permeation is determined in the absence of K^+ ions, we find that both W434F channels and C-type inactivated *Sh*Δ channels show maintained Na^+ and Li^+ currents, although both are functionally impermeant to K^+ ions.

(c) Activation of Na^+ currents through W434F channels is unusually slow (see Fig. 3 B) and the rate-limiting time constant is ~20 ms even at +100 mV test po-

tential. Similarly, Na^+ current activation in C-type inactivated $Sh\Delta$ channels is slower than in noninactivated $Sh\Delta$ channels (see Fig. 8 of Starkus et al., 1997). Additionally, the similarity in deactivation rates between W434F and C-type inactivated $Sh\Delta$ channels is shown in Fig. 4. Thus, there are marked kinetic similarities between W434F channels and C-type inactivated $Sh\Delta$ channels, while the kinetics of activation and deactivation in W434F differ markedly from those of noninactivated $Sh\Delta$.

(*d*) Although $Sh\Delta$ Na^+ tail currents show clear evidence (see Fig. 1 *C*) of the development of C-type inactivation during the first 50–100 ms of the depolarizing test pulse, any time-dependent changes in W434F tail currents (see Fig. 1 *D*) are small and detectable only at the shortest test pulse duration used here (2 ms). If the slow activation and deactivation kinetics of Na^+ currents in W434F channels result from C-type inactivation, then this inactivated state is either "permanent" or entered very early during a depolarizing pulse.

Overall, the evidence presented here indicates a close resemblance between both the kinetics and selectivity of W434F and $Sh\Delta$ channels, once $Sh\Delta$ channels have entered a C-type inactivated state. The most economical interpretation of these findings would be that W434F channels are indeed permanently C-type inactivated at depolarized potentials, as suggested from different lines of evidence by Yang et al. (1997). Although the evidence presented here and by Yang et al. (1997) seems both detailed and strong, the conclusion that W434F channels are permanently C-type inactivated has been challenged by Olcese et al. (1997). These authors show that the time course of development of C-type inactivation in *Shaker* H4-D parallels the rate of left-shifting of the charge–voltage [Q(V)][1] distribution in the W434F mutant. Furthermore, both C-type inactivation and the Q(V) left-shift recover with similar rates when both parameters are evaluated in *Shaker* H4-D channels. They conclude that the rate of Q(V) left shifting is a valid indicator of the rate of development of C-type inactivation and, hence, that W434F enters C-type inactivation only very slowly under the conditions used for their experiments.

The apparent conflict between the conclusions of Olcese et al. (1997) and those reached here arises from the use of different surrogate methods for identification of C-type inactivation in nonconducting W434F channels. Unfortunately, the gold-standard for C-type inactivation remains time-dependent changes in macroscopic K^+ currents, which cannot be readily assessed in the W434F mutant. However, Yang et al. (1997) have reported a time constant of ∼1 ms for the disappear-

ance of K^+ permeation in depolarized W434F channels, based on ensemble averages of single channel measurements, which, as might be expected, occurred only with very low probability in their data but always very early in the depolarizing step.

C-type inactivation is a slow process in physiological solutions, and becomes even slower when $[K^+]_o$ is increased. On the other hand, C-type inactivation of K^+ permeation becomes increasingly fast with reduction of $[K^+]_o$ (López-Barneo et al., 1993) and/or $[K^+]_i$ (Starkus et al., 1997; Kiss and Korn, 1998). As a result, K^+ sensitivity has been used as a diagnostic criterion for the presence of C-type inactivation in Kv1.4 (Rasmusson et al., 1995) and HERG (human *ether-à-go-go*-related gene; Schönherr and Heinemann, 1996) channels. It follows that no parameter should be selected as an indirect marker for C-type inactivation unless this parameter continues to track the development of C-type inactivation when solutions of differing ionic content impose widely differing inactivation rates. Only then can some mechanistic link be assumed between the selected indirect indicator and C-type inactivation, as determined from the inactivation of macroscopic K^+ currents. The development of slow Na^+ tail currents meets this criterion in $Sh\Delta$ channels. Slow Na^+ tail currents develop within 60 ms in K^+-free Na^+ solutions where C-type inactivation is also complete by this time. Furthermore, development of slow Na^+ tail currents correlates with development of C-type inactivation in external Normal Frog Ringer, where C-type inactivation requires 2 s to equilibrate (compare Figs. 2 and 3 of Starkus et al., 1997). By this criterion of slow Na^+ tail currents, W434F channels appear fully C-type inactivated at, or before, the time of channel opening (see Fig. 1). Thus, the slow left shift in the Q(V) curve noted by Olcese et al. (1997) may reflect some other aspect of the complex slow inactivation mechanisms of voltage-gated potassium channels.

In previous work using $Sh\Delta$ channels, the rates of deactivation and OFF charge return could have been affected in three different ways: (*a*) by effects of ionic conditions on channel state (since, as noted above, C-type inactivation rates are highly susceptible to changes in $[K^+]_o$ and $[K^+]_i$), (*b*) by more direct effects of permeating ions (Zagotta et al., 1994), or (*c*) by removal of K^+ ions from some internal regulatory site. After the ground breaking work of Chen et al. (1997), showing that ionic conditions have greater effects on deactivation kinetics than had previously been recognized, we exploited the apparently constitutive nature of C-type inactivation in W434F channels to remove the first of the above variables: change of channel state. We show here (see Fig. 5) that the principal time constant for return of OFF gating charge in W434F channels changes from 1.6 to 16 ms when K^+-containing physiological solutions are substituted by K^+-free solutions supporting

[1]*Abbreviation used in this paper:* charge-voltage, Q(V).

Na$^+$ tail currents. Furthermore, under these conditions the return of OFF charge appears tightly coupled to the rate of ionic current deactivation. While it seems clear that the observed slowing of gating charge return results from the change in ionic conditions, more work will be required to clarify whether this is a permeant ion effect, a regulatory effect of K$^+$ binding, or whether both actions may be involved in this effect.

Finally, Starkus et al. (1997) have hypothesized that the selectivity change characteristic of C-type inactivation results from an inherently fast conformational change that is triggered whenever K$^+$ ions are absent from the selectivity filter of an open *Sh*Δ channel for more than some short critical interval (see also Baukrowitz and Yellen, 1996). More recently, Kiss and Korn (1998) have provided additional evidence associating the site at which K$^+$ ions regulate development of C-type inactivation with the selectivity filter itself, rather than with more superficially placed sites. We speculate, therefore, that the W434F mutation alters the structure of the selectivity filter and substantially reduces its affinity for K$^+$ ions. This action alone might be sufficient to create a channel that is, in effect, permanently C-type inactivated.

REFERENCES

Baukrowitz, T., and G. Yellen. 1996. Use-dependent blockers and exit rate of the last ion from the multi-ion pore of a K$^+$ channel. *Science.* 271:653–656.

Bezanilla, F., and E. Stefani. 1994. Voltage-dependent gating of ionic channels. *Annu. Rev. Biophys. Biomol. Struct.* 23:819–846.

Chen, F.S.P., D. Steele, and D. Fedida. 1997. Allosteric effects of permeating cations on gating currents during K$^+$ channel deactivation. *J. Gen. Physiol.* 110:87–100.

Hamill, O.P., A. Marty, E. Neher, B. Sakmann, and F.J. Sigworth. 1981. Improved patch-clamp techniques for high-resolution current recording from cells and cell-free membrane patches. *Pflügers Arch.* 391:85–100.

Heinemann, S.H., F. Conti, and W. Stühmer. 1992. Recording of gating currents from *Xenopus* oocytes and gating noise analysis. *Methods Enzymol.* 207:353–368.

Iverson, L.E., and B. Rudy. 1990. The role of divergent amino and carboxyl domains on the inactivation properties of potassium channels derived from the *Shaker* gene of *Drosophila. J. Neurosci.* 10:2903–2916.

Kiss, L., and S.J. Korn. 1998. Modulation of C-type inactivation by K$^+$ at the potassium channel selectivity filter. *Biophys. J.* 74:1840–1849.

Korn, S.J., and S.R. Ikeda. 1995. Permeation selectivity by competition in a delayed rectifier potassium channel. *Science.* 269:410–412.

Liu, Y., M.E. Jurman, and G. Yellen. 1996. Dynamic rearrangement of the outer mouth of a K$^+$ channel during gating. *Neuron.* 16:859–867.

López-Barneo, J., T. Hoshi, S.H. Heinemann, and R.W. Aldrich. 1993. Effects of external cations and mutations in the pore region on C-type inactivation of *Shaker* potassium channels. *Receptors Channels.* 1:61–71.

McCormack, K., W.J. Joiner, and S.H. Heinemann. 1994. A characterization of the activating structural rearrangements in voltage-dependent *Shaker* K$^+$ channels. *Neuron.* 12:301–315.

Olcese, R., R. Latorre, L. Toro, F. Bezanilla, and E. Stefani. 1997. Correlation between charge movement and ionic current during slow inactivation in *Shaker* K$^+$ channels. *J. Gen. Physiol.* 110:579–589.

Perozo, E., R. MacKinnon, F. Bezanilla, and E. Stefani. 1993. Gating currents from a nonconducting mutant reveal open-closed conformations in *Shaker* K$^+$ channels. *Neuron.* 11:353–358.

Rasmusson, R.L., M.J. Morales, R.C. Castellino, Y. Zhang, D.C. Campbell, and H.C. Strauss. 1995. C-type inactivating cardiac K+ channel (Kv1.4) expressed in *Xenopus* oocytes. *J. Physiol. (Camb.).* 489:709–721.

Schlief, T., R. Schönherr, and S.H. Heinemann. 1996. Modification of C-type inactivation *Shaker* potassium channels by chloramine-T. *Pflügers Arch.* 431:483–493.

Schönherr, R., and S.H. Heinemann. 1996. Molecular determinants for activation and inactivation of HERG, a human inward rectifier potassium channel. *J. Physiol. (Camb.).* 493:635–642.

Starkus, J.G., L. Kuschel, M.D. Rayner, and S.H. Heinemann. 1997. Ion conduction through C-type inactivated *Shaker* channels. *J. Gen. Physiol.* 110:539–550.

Yang, Y., Y. Yan, and F.J. Sigworth. 1997. How does the W434F mutation block current in *Shaker* potassium channels? *J. Gen. Physiol.* 109:779–789.

Zagotta, W.N., T. Hoshi, J. Dittman, and R.W. Aldrich. 1994. *Shaker* potassium channel gating. II: Transition in the activation pathway. *J. Gen. Physiol.* 103:279–319.